International Journal of Basic and Applied Sciences, 12 (1) (2023) 14-21

International Journal of Basic and Applied Sciences

Website: www.sciencepubco.com/index.php/IJBAS

Research paper

Parametric identification method for an absorption air conditioning parabolic trough collector solar plant

J. Díaz-Salgado [1], S. García-López [1], Y. R. Galindo-Luna [2,*], R. J. Romero [3]

[1] *División de Ingeniería Mecatrónica e Industrial, Tecnológico de Estudios Superiores de Ecatepec, Edo. de México*
[2] *Universidad Autónoma Metropolitana-Iztapalapa.Av. Ferrocarril San Rafael Atlixco 186, Col. Leyes de Reforma 1A Sección, Iztapalapa, C.P. 09310, Ciudad de México, México.*
[3] *Centro de Investigación en Ingeniería y Ciencias Aplicadas, Universidad Autónoma del Estado de Morelos, Av. Universidad 1001, Cuernavaca, Morelos, CP 62209, México*
**Corresponding author E-mail:* ygalindo@izt.uam.mx

Abstract

In this work is established a parametric identification method for an absorption air conditioning solar plant. A scaled thermal plant, consisting of a thermal capacitor and a flow line that acts as a capacitor and thermal energy radiator is used. As the mathematical model of the scaled plant is structurally identical to that of the solar plant the first is used to determine the methodology that can be used later for the identification of the PTC solar plant. Parametric identification is a necessary step that allows to determine the unknown parameters of the mathematical model of any solar/thermal plant. This model then can be used to analyze the plant characteristics and design an appropriate control algorithm. Although the system model is nonlin-ear it can be expressed in the form of a linear regressor in the parameters. This permits to use the least squares method as the identification method. The method is applied to the thermal plant to identify the useful form that the covariance matrix and excitation signals should have to ensure that when applied to the solar plant its unknown parameters can be properly estimated. Once the solar plant parameters are properly estimated model can be used to analyze and simulate the operation of the ab-sorption air conditioning system.

Keywords: *Recursive Identification; Process Modeling and Identification.*

1. Introduction

In recent years, different medium and high temperature solar thermal systems applied to cooling and/or air conditioning have been developed (Al-Alili et al., 2014; Tashtoush & Nayfeh, 2020). Commonly the solar air conditioning systems (by absorption or adsorption) have been coupled with a solar plant that is responsible for capturing and storing thermal energy and then transferring it to the thermodynamic cooling system (Braun et al., 2020; Mathur, 2020) There are various types of solar collectors, however, the use of medium temperature absorption systems has preferred the use of parabolic trough collectors (Siddiqui & Said, 2015). These concentrators use a heating fluid, which flows through a receiving tube, increasing the temperature of the fluid to achieve the thermal level required by the thermodynamic cycle and can reach up to 400°C. The working fluid is introduced to the thermodynamic cycle and/or stored in an insulated tank, which functions as a thermal capacitor. The output temperature of a solar plant must be kept within a narrow design range to ensure proper operation of the thermodynamic cycle. However, it suffers from three important disturbances that must be compensated by any control system: (i) solar irradiation changes throughout the day, (ii) the workflow inlet temperature and (iii) climatic conditions (mainly changes in ambient temperature) (Lemos, 2006) The design of the temperature regulation control requires an adequate and accurate mathematical model (E. F. Camacho et al., 2007; E.F. Camacho et al., 1992) However, in particular in solar plant models, the thermal losses and collectors optical efficiency coefficients are difficult to determine. One way to achieve this is through a certification service that involves a high economic cost since experimental tests are carried out with a very specialized equipment. To overcome this problem several methods (static method, dynamic method, or artificial intelligence-based methods) have been used for solving the problem of parameter estimation (Askarzadeh & Gharibi, 2018; Secui et al., 2020). The least squares method is a current recursive method that stands out among other methods and can be applied to linear and nonlinear systems.

Recently a cooling system for air-conditioning pilot plant has been designed in CIICAp, Mexico (Luna, 2018). The designed solar thermal cooling system is an absorption NaOH-H2O cycle type with an energy demand of 6,600 kW/h with a nominal operation temperature of 94°C. The aim of this research is to design a regulation controller that maintain this temperature as closer as possible to the nominal value. For this purpose is necessary to establish an adequate solar plant model, thus the motivation of this study is to establish an appropriate methodology to design a parameter estimator of the unknown model parameters of the solar thermal plant. As a point of departure this work uses the recursive least squares method to indirectly determine thermal loss coefficients from experimental data from a thermal plant

that has structurally identical behavior to that of the solar thermal plant. Once established this methodology will be applied to the solar plant.
The main interest of this work is focused on : (i) determining whether the system excitation inputs are rich enough to estimate unknown parameters, (ii) establishing a covariance matrix of the parametric estimation algorithm suitable for a thermal plant and (iii) determining from two very similar plant models which one improves the parameter estimation. The work is organized as follows: first the solar and thermal plant are described and two mathematical models are proposed, next the recursive parametric estimation algorithm and the error criteria used to compare the estimated parameters are described, the next section describes the characteristics of the experimental tests performed, then the experimental results are shown, and finally the conclusions of the work are presented.

2. Plant description

2.1. Description of the solar thermal plant

The solar thermal plant (Fig. 1).

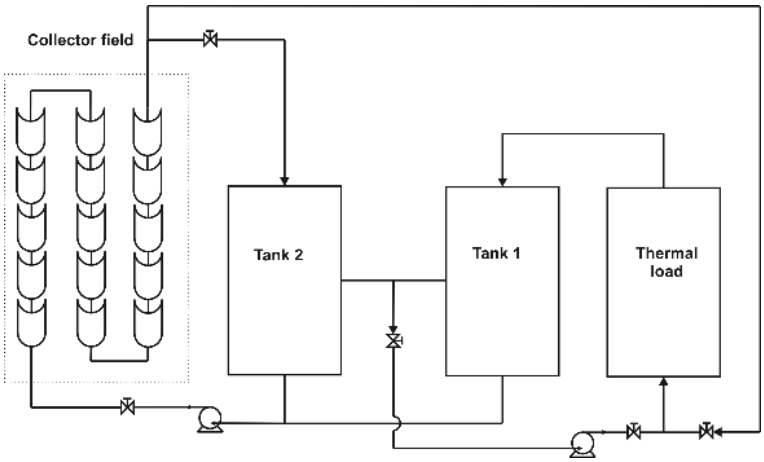

Fig. 1: Solar Thermal Plant Diagram.

The PTC solar plant (Fig. 1) is composed of a collector field, two thermal storage tanks, two pumps and the valves and flow lines that interconnect the system elements. Meanwhile, the distributed solar collector field is composed of 15 units of parabolic mirrors with a total mirror surface of 40.05 m2. The constant flow is forced with two pumps that delivers a maximum of 36.5 l/min. The solar thermal plant is dimensioned to provide the 6,600 kW-h needed by the air conditioning system at a nominal temperature of 94°C. A complete description of the plant can be founded in (Diaz-Salgado J. et al., 2017; Luna, 2018)

2.2. Description of the thermal plant

The scaled thermal plant (Fig. 2) consists of a 15 liters capacity storage tank, a 3/4 inch 20 m length hose with 5.58 kg of capacity, an electric heating unit that transfers thermal energy to the inlet of the flow line and a pump that regulates the flow of the system acting as the control element. The plant is instrumented with four thermocouples that measure the flow line temperature (TT1), the heating unit inlet and outlet temperatures (TT2 and TT3) and the ambient temperature (TT4). It also features an RTD probe that measures the temperature at the bottom of the tank (TT5) and a turbine flow meter (FT1). Using an electronic interface (FIC1), the speed of a DC pump (SC1) and the power of the heating unit can be manipulated by means of PWM signals.

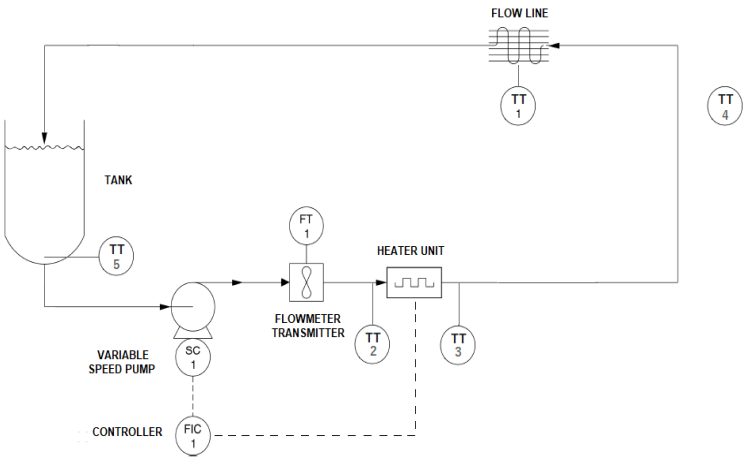

Fig. 2: Scaled Thermal Plant Diagram.

2.3. Mathematical model

Taking into account only Tank 2 of the solar plant (Fig. 1), and departing from the specialized literature (Eduardo F. Camacho et al., 2014; Duffie et al., 2013) heat transfer and thermal balance equations a lumped parameter model (1) is proposed for the solar plant considering the flow line (T_l) and storage tank (T_T) temperatures

$$\dot{T}_l = \frac{\eta_0 S}{c_l} I - \frac{\dot{q}\rho c_p}{c_l}(T_l - T_T) - \frac{H_l}{c_l}(T_l - T_a) \quad (1a)$$

$$\dot{T}_T = \frac{\dot{q}\rho c_p}{c_T}(T_l - T_T) - \frac{H_T}{c_T}(T_T - T_a) \quad (1b)$$

The first term of the flow line temperature dynamics (1a) considers the irradiated solar energy over the collector field, the second term corresponds to the thermal energy transferred from the flow line to the storage tank, while the last term considers the loss of thermal energy to the environment. On the other hand, the first term of the temperature dynamics of the storage tank (1b) considers the thermal energy received from the flow line and the second term the environment thermal losses. The system inputs are the ambient temperature T_a, the solar irradiance I, and the input flow rate $\dot{q}$, the two first are considered as measured disturbances and the latter as the control input. The plant parameters are: (i) the working fluid specific heat c_p, (ii) the working fluid density ρ, (iii) the dimensionless optical efficiency coefficient η_0, (iv) the solar concentration area A, (v) the flow line and thermal tank thermal capacitances (c_l and c_T respectively) that are defined as the heat flow necessary to change the temperature rate of a medium by one unit in one second, and are calculated from the product of specific heat capacity and the mass of the respective capacitor (2), and (vi) the flow line and thermal tank thermal losses (H_l and H_T respectively) defined as total transfer of heat through the capacitor to the ambient either from conduction, convection, radiation, or any combination of the these.

The scaled thermal plant model (2) has the same tank temperature dynamic and only differs from the solar plant in the first term of the flow line dynamic (2a). The irradiated solar energy over the collector field changes to the thermal energy transferred by the electric heater. This means: (i) the input of the thermal plant is the heater input voltage V instead of the solar irradiance I, and (ii) the optical efficiency coefficient and solar concentration area product $\eta_0 S$ changes to the heater thermal constant h_T that is defined as the power delivered from the heater unit in terms of the applied voltage,

$$\dot{T}_l = \frac{h_T}{c_l} V - \frac{\dot{q}\rho c_p}{c_l}(T_l - T_T) - \frac{H_l}{c_l}(T_l - T_a) \quad (2a)$$

$$\dot{T}_T = \frac{\dot{q}\rho c_p}{c_T}(T_l - T_T) - \frac{H_T}{c_T}(T_T - T_a) \quad (2b)$$

Table 1: Nomenclature

Symbol	Name	Units
T_l	line temperature	C
T_T	tank temperature	C
T_a	ambient temperature	C
V	heater input voltage	V
I	solar irradiance	W/m^2
$\dot{q}$	input flow rate	lt/min
η_0	optical efficiency coefficient	[/]
S	solar concentration area	m^2
c_p	working fluid specific heat	J/kg-C
ρ	working fluid density	Kg/m^3
c_l	flow line thermal capacitance	J/C
c_T	storage tank thermal capacitance	J/C
h_T	heater thermal constant	W/V
H_l	flow line thermal losses	W/C
H_T	storage tank thermal losses	W/C

2.4. Alternative mathematical model

In the solar thermal plants specialized literature the term of loss of thermal energy of the flow line to the environment considers the difference between the average temperature (of the tank and the flow line) and the environment, instead of using the difference between line temperature and the environment, ensuring that this improves the fidelity of the model (Berenguel et al., 2012). Extrapolating this recommendation to the thermal plant an alternative model is proposed (3). The purpose of including this alternative model is to determine if this difference improves the parameter estimation.

$$\dot{T}_l = \frac{h_T}{c_l} V - \frac{\dot{q}\rho c_p}{c_l}(T_l - T_T) - \frac{H_l}{c_l}\left[\frac{(T_l + T_T)}{2} - T_a\right] \quad (3a)$$

$$\dot{T}_T = \frac{\dot{q}\rho c_p}{c_T}(T_l - T_T) - \frac{H_T}{c_T}(T_T - T_a) \quad (3b)$$

The difference between the model (2) and the alternative model (3) lies in the third term of the flow line temperature dynamics (3a).

3. Parameter identification

3.1. Recursive identification algorithm

The least squares (Karl J. Astrom, 1994) identification method can be used in nonlinear models such as the one presented by the plant provided that it can be expressed in the form of a parameter linear regressor. In this way, the least squares recursive algorithm requires the mathematical model of the plant to be rewritten in the parameter linear form:

$$y(k) = \psi(k)^T \theta \tag{4}$$

Where $y(k) \epsilon \mathbb{R}^n$ it is the measurement output vector, $\psi(k) \mathbb{R}^{pxn}$ is the regression matrix whose data is known as they are the functions of the model evaluated with experimental data and $\theta \epsilon \mathbb{R}^p$ is the unknown parameter vector. The least squares recursive algorithm is the follow:

$$\hat{\theta}(k) = \hat{\theta}(k-1) + P(k-1)\psi(k)[I + \psi(k-1)^T P(k-1)\psi(k)]^{-1} e(k) \tag{5a}$$

$$P(k) = P(k-1) - P(k-1)\psi(k)[I + \psi(k)^{-T} P(k-1)\psi(k)]^{-1} \psi(k)^T P(k-1) \tag{5b}$$

$$e(k) = y(k) - \psi(k)^T \hat{\theta}(k-1) \tag{5c}$$

Where $P(k) \epsilon \mathbb{R}^{pxp}$ it is the covariance matrix, $e(k) \epsilon \mathbb{R}^n$ it is the error prediction, and $\hat{\theta}(k)$ it is the estimated parameter vector.

3.2. Plant model expressed in parameter linear form

If the thermal plant model (3) is rewritten in the parameter linear form (4) using the regression matrix of 5x2 (6a), the output vector of 2x1 (6b) and the 5x1 (6c) parameter vector it is possible to determine the two unknown parameters of the plant (H_l, H_T) from the known $(c_p, \rho, c_l, c_T, h_T)$ ones because the elements $\theta_{1,1}$, $\theta_{2,1}$ and $\theta_{4,1}$ of the parameter vector are known.

$$\psi(k)^T = \begin{bmatrix} V & -\dot{q}(T_l - T_T) & -(T_l - T_a) & 0 & 0 \\ 0 & 0 & 0 & \dot{q}(T_l - T_T) & -(T_T - T_a) \end{bmatrix} \tag{6a}$$

$$y(k) = [\dot{T}_l \quad \dot{T}_T]^T \tag{6b}$$

$$\theta = \left[\frac{h_T}{c_l} \quad \frac{\rho c_p}{c_l} \quad \frac{H_l}{c_l} \quad \frac{\rho c_p}{c_T} \quad \frac{H_T}{c_T}\right]^T \tag{6c}$$

3.3. Absolute error sum criteria

The Absolut Error Sum criteria (7) defined as the sum of the absolute value of the differences between actual y_i and estimated $\hat{y}_i$ output values is a quantitative weighting tool proposed to compare between different parameter estimation algorithms in order to obtain a quantitative result (Secui et al., 2020). In this work, the AES criteria is used to compare the estimated parameters between the two considered plant models (2) and (3).

$$AES = \sum_{i=1}^{N} |y_i - \hat{y}_i| \tag{7}$$

Where N is the number of observations (outputs).

4. Experimental tests

The parametric estimation method is applied to the data obtained from two different experimental tests which characteristics are detailed. Both tests were designed to be applied in the solar thermal plant.

4. 1. Description of test 1

Test 1 (Fig. 3) lasted approximately 12:36 hrs. A 3V constant control signal is introduced to the pump during the first 5000 s (approx. 1:20 hrs.) resulting in an almost constant flow rate of around 5 lt/min, also a constant voltage of 3V is introduced to the electric heater. After this time both actuators are turned off waiting for the plant to achieve a thermal balance (approx. 11:10 hrs).

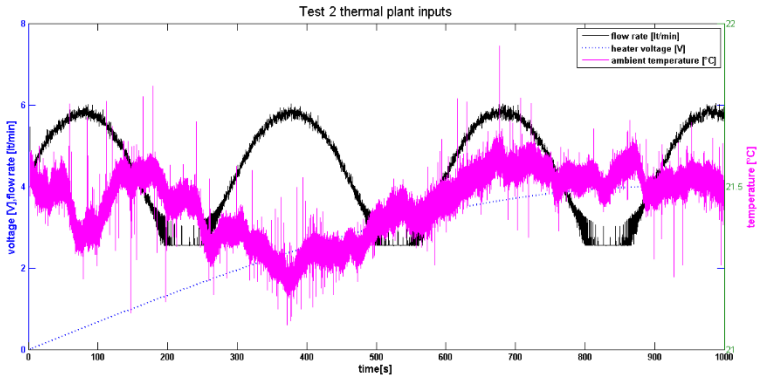

Fig. 3: Test 1 Plant Inputs.

4. 2. Description of test 2

Test 2 (Fig. 4) lasted approximately 26 min. A sinusoidal signal was introduced to the pump to obtain a flow rate with a of 4 l/min direct component, 2 l/min amplitude and 300 s period, while the voltage signal of the heater corresponds to the transformed in amplitude and time signal from W/m^2 to W/V of the solar irradiation presented on November 23, 2017 in Cuernavaca Mor.

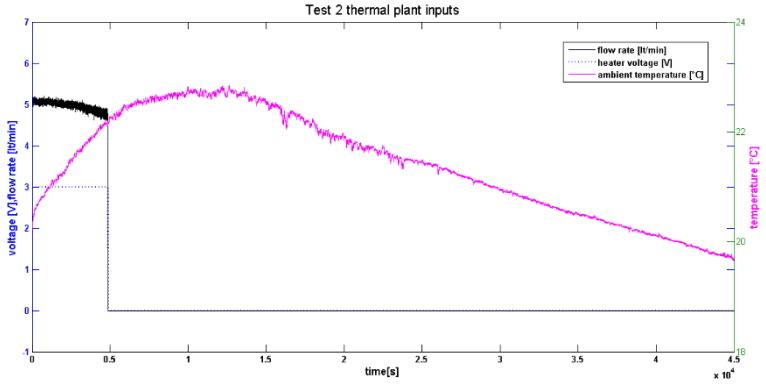

Fig. 4: Test 2 Plant Inputs.

5. Results

5. 1 Thermal loss coefficients assessment

In order to establish reference values, the parametric estimation algorithm is applied to the experimental data of Test 1 from the second 5001 (i.e. in a quasi-dynamic regime), which simplifies the model (1) to:

$$\dot{T}_l = -\frac{H_l}{c_l}(T_l - T_a) \tag{7a}$$

$$\dot{T}_T = -\frac{H_T}{c_T}(T_T - T_a) \tag{7b}$$

By doing so, and proposing the regression matrix (8a), the output vector (8b) and the parameter vector (8c) it is possible to estimate the parameters (H_l, H_T).

$$\psi(k)^T = \begin{bmatrix} -(T_l + T_a) \\ -(T_T - T_a) \end{bmatrix} \tag{8a}$$

$$y(k) = [\dot{T}_l \quad \dot{T}_T]^T \tag{8b}$$

$$\theta = \begin{bmatrix} \frac{H_l}{c_l} & \frac{H_T}{c_T} \end{bmatrix}^T \tag{8c}$$

Moreover, in virtue that the parameters (c_l, c_T) are known to improve the estimation accuracy the model (8) is modified to the (9) one that allows to directly estimate the coefficients of thermal losses.

$$\psi(k)^T = \begin{bmatrix} -\frac{1}{c_l}(T_l + T_a) \\ -\frac{1}{c_T}(T_T - T_a) \end{bmatrix} \tag{9a}$$

$$y(k) = [\dot{T}_l \quad \dot{T}_T]^T \tag{9b}$$

$$\theta = [H_l \; H_T]^T \tag{9c}$$

The described procedure is repeated for the alternative model (3) obtaining a set of estimated parameters with both models (Table 2). The average of both is used as a reference value to compare this parameters vs those estimated with the model (6) and the complete experimental data in Test 1 (Table 3).

Table 2: Estimated Parameters

Parameterized model	Plant Model	H_l	H_T
Model (7)	Model (1)	2.20	8.17
	Model (3)	0.95	8.17
Model (8)	Model (1)	2.19	7.47
	Model (3)	1.68	7.47
Average	Model (1)	2.19	7.82
	Model (3)	1.32	7.82

The results in Table 3 show that both mathematical models (2) and (3) behave similarly with a maximum error of 20.54 and 32.17% with respect to the average of the parameters estimated in the quasi-dynamic regime of Test 1, showing good concordance between the two regimes.

Table 3: Estimated Parameters Sets with Parametric Model (5) and Test 1

Parameter	θ_1	θ_2	θ_3	θ_4	θ_5
Physical parameters	$\frac{h_T}{c_l}$	$\frac{\rho c_p}{c_l}$	$\frac{H_l}{c_l}$	$\frac{\rho c_p}{c_T}$	$\frac{H_T}{c_T}$
Model (2)	1.00	0.96	1.74	0.99	8.03
error %	0.00	4.00	20.54	1.00	2.68
Ref. model (2)	1.00	1.00	2.19	1.00	7.82
Model (3)	1.00	0.99	1.87	0.99	8.03
error %	0.00	1.00	32.17	0.01	2.68
Ref. model (3)	1.00	1.00	1.32	1.00	7.82

5. 2 Model parameters assessment

The estimation algorithm (4) is applied with the parameterized model (5), the data of both tests (Test 1 and 2) and considering the difference between both models (1) and (3) in the regression matrix (5a). In this way, four sets of estimated parameters are obtained that are named: A to that obtained with the data from test 1 with the model (2), B corresponds to test 1 with model (3), C corresponds to test 2 with model (2) and D corresponds to test 2 with model (3). The values of the 5x5 covariance matrix used (9) were proposed iteratively. Departing from the identity matrix, their values were modified by comparing the obtained parameters against the reference values (Table 3) until reaching the reported values where a maximum error value of 32.17% is achieved. The guideline used to find appropriate values of the regression matrix (10) was to give greater weight to the unknown parameters $\theta_{3,1}$ and $\theta_{5,1}$ with respect to the known ones, $\theta_{1,1}$, $\theta_{2,1}$and $\theta_{4,1}$.

$$P = \begin{bmatrix} 0.001 & 0 & 0 & 0 & 0 \\ 0 & .001 & 0 & 0 & 0 \\ 0 & 0 & 1 & 0 & 0 \\ 0 & 0 & 0 & .001 & 0 \\ 0 & 0 & 0 & 0 & 1 \end{bmatrix} \tag{10}$$

After several iterations, it was determined that a difference in weight of three orders of magnitude is very suitable. Reference values were also used as initial conditions of the estimated parameter vector (5a). To quantitatively determine the best set of parameters, the AES criteria of the error generated by the difference between the experimental and the simulated values (Figs 5-8) are determined for each set of parameters and both tests (Table 4 and Figs. 9 and 10).

Table 4: AES Estimation Error Criteria

Test	Parameters	AES
1	A	143.3
	B	93.25
	C	480.78
	D	645.72
2	A	2.1716
	B	2.0459
	C	3.4006
	D	2.8252

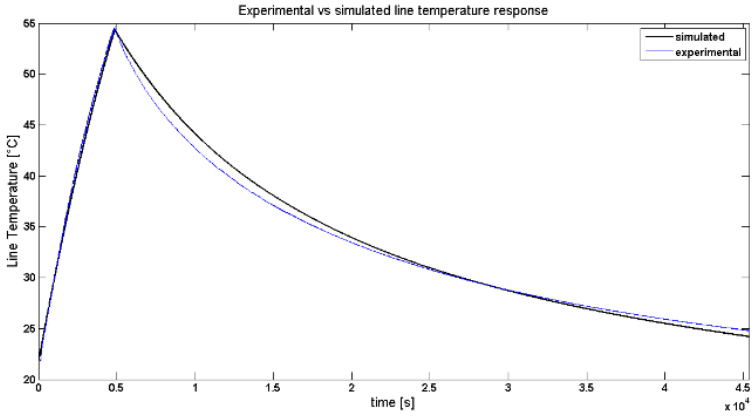

Fig. 5: Experimental Vs Simulated T_l with Test 1 And Set B.

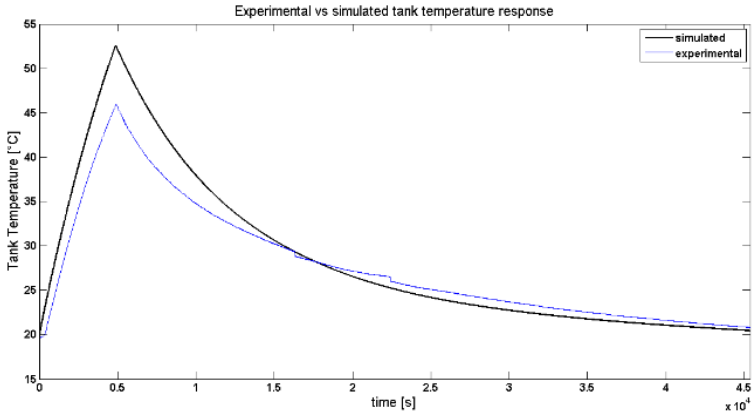

Fig. 6: Experimental vs Simulated T_T with Test 1 and Set B.

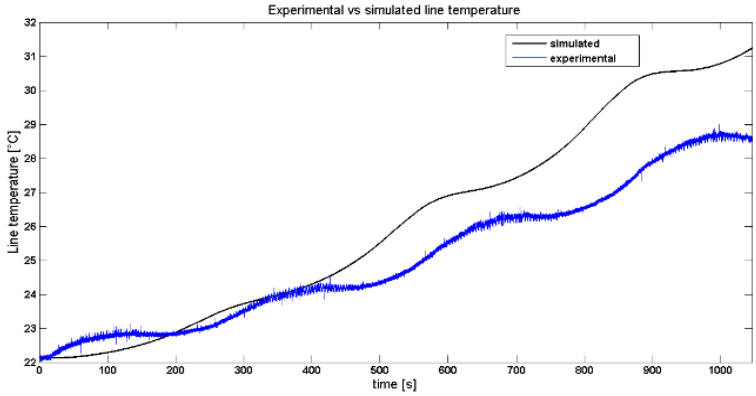

Fig. 7: Experimental vs Simulated T_l with Test 2 And Set B.

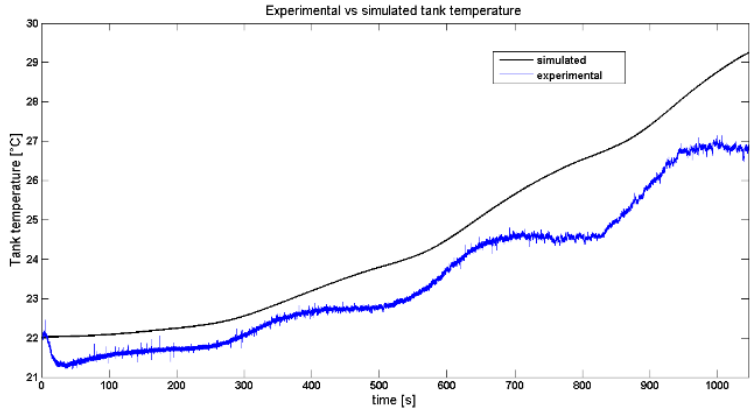

Fig. 8: Experimental vs Simulated T_T with Test 2 and Set B.

The AES criteria allows to conclude that the best set of parameters are B because presents the less value between the other parameter sets for both tests.

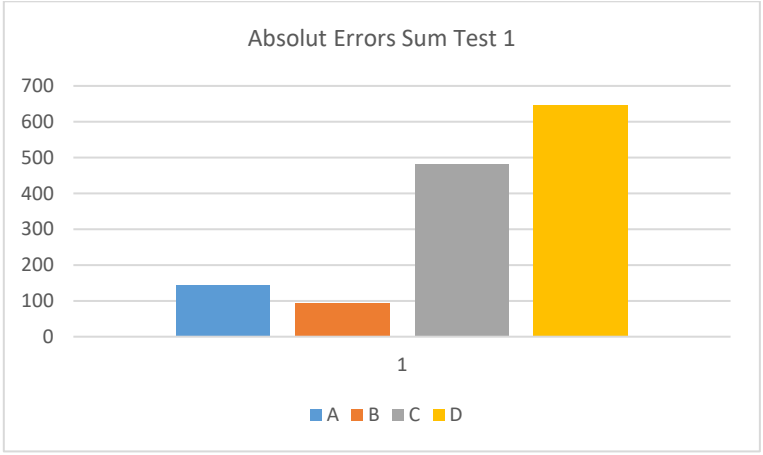

Fig. 9: AES Error Criteria for Test 1.

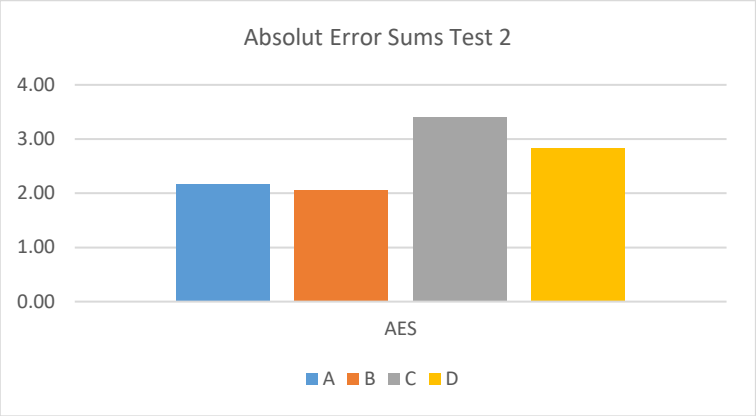

Fig. 10: AES Error Criteria for Test 2.

6. Conclusions

The recursive least squares algorithm was applied to experimental data obtained from two tests designed purposely to indirectly estimate the unknown parameters of two dynamic models of a thermal plant. Parameter reference values were estimated first from the quasi-dynamic regime of the plant and compared against the dynamic regime ones showing good concordance between the two parametric estimates. This also allowed: (i) to propose an appropriate regression matrix for parametric estimation and (ii) to set the initial conditions of the estimated parameters vector using the reference values. Finally, four sets of estimated parameters were obtained by comparing their simulated vs experimental behavior among two different dynamic tests. From this comparison and the computation of the AES criteria error it can be concluded that the best set of parameters was determined from the data of Test 1 and the alternative model since it presents the lowest AES criteria. Future work consists in applying the same methodology and tests to a solar thermal plant whose mathematical model is structurally identical to that of the thermal plant, assuming that doing so will allow a proper estimation of the coefficients of thermal losses and optical efficiency of solar collectors that are the commonly unknown parameters of a solar plant.

References

[1] Al-Alili, A., Hwang, Y., & Radermacher, R. (2014). Review of solar thermal air conditioning technologies. *International Journal of Refrigeration*, *39*, 4–22. https://doi.org/10.1016/j.ijrefrig.2013.11.028.

[2] Askarzadeh, A., & Gharibi, M. (2018). Accurate estimation of cost function parameters for thermal power plants using a novel optimization approach. *Energy Sources, Part A: Recovery, Utilization and Environmental Effects*, *40*(24), 2986–2999. https://doi.org/10.1080/15567036.2018.1514440.

[3] Berenguel, M., Rubio, F. R., Martínez, D., & Camacho, E. F. (2012). Control of solar energy systems. In *Advances in industrial control*. https://doi.org/10.1007/978-0-85729-916-1.

[4] Braun, R., Haag, M., Stave, J., Abdelnour, N., & Eicker, U. (2020). System design and feasibility of trigeneration systems with hybrid photovoltaic-thermal (PVT) collectors for zero energy office buildings in different climates. *Solar Energy*, *196*(March 2019), 39–48. https://doi.org/10.1016/j.solener.2019.12.005.

[5] Camacho, E. F., Rubio, F. R., Berenguel, M., & Valenzuela, L. (2007). A survey on control schemes for distributed solar collector fields. Part I: Modeling and basic control approaches. *Solar Energy*, *81*(10), 1240–1251. https://doi.org/10.1016/j.solener.2007.01.002.

[6] Camacho, E.F., Rubio, F. R., & Hughes, F. M. (1992). Self-tuning control of a solar power plant with a distributed\ncollector field. In *Control Systems, IEEE* (Vol. 12, Issue 2, pp. 72–78). https://doi.org/10.1109/37.126858.

[7] Camacho, Eduardo F., Berenguel, M., & Gallego, A. J. (2014). Control of thermal solar energy plants. *Journal of Process Control*, *24*(2), 332–340. https://doi.org/10.1016/j.jprocont.2013.09.026.

[8] Diaz-Salgado J., Basurto-Pensado, M. A., & R.J., R. (2017). Diseño y Dimensionamiento del Actuador de un Sistema de Seguimiento Solar de un Colector Cilindro-Parabólico para una Planta Solar de Aire Acondicionado Utilizando Herramientas de Simulación por Software Design and power calculation of the Sun Tracking Sy. *Programación Matemática y Software*, *9*, 1–9. https://doi.org/10.30973/progmat/2017.9.3/1.

[9] Duffie, J. a., Beckman, W. a., & Worek, W. M. (2013). Solar Engineering of Thermal Processes, 4nd ed. In *Journal of Solar Energy Engineering* (Vol. 116). https://doi.org/10.1115/1.2930068.

[10] Karl J. Astrom, B. W. (1994). Adaptive Control. In *Dover*.

[11] Lemos, J. M. (2006). Adaptive control of distributed collector solar fields. *Internatioal Journal of Systems Science*, *37*(January 2014), 523–533. https://doi.org/10.1080/00207720600783686.

[12] Luna, Y. R. G. (2018). *Diseño, construcción y evaluación experimental de una planta piloto solar para acondicionamiento de espacio utilizando la mezcla NaOH-H20 para climas cálidos subhúmedos*.

[13] Mathur, D. (2020). *A REVIEW ON SOLAR COOLING*. *11*(5), 12–21. https://doi.org/10.34218/IJMET.11.5.2020.002.

[14] Secui, D. C., Hora, C., Bendea, G., & Bendea, C. (2020). Parameter estimation using a modified whale optimization algorithm for input-output curves of thermal and hydro power plants. *International Transactions on Electrical Energy Systems*, *30*(2). https://doi.org/10.1002/2050-7038.12188.

[15] Siddiqui, M. U., & Said, S. A. M. (2015). A review of solar powered absorption systems. *Renewable and Sustainable Energy Reviews*, *42*, 93–115. https://doi.org/10.1016/j.rser.2014.10.014.

[16] Tashtoush, B., & Nayfeh, Y. (2020). Energy and economic analysis of a variable-geometry ejector in solar cooling systems for residential buildings. *Journal of Energy Storage*, *27*(November 2019), 101061. https://doi.org/10.1016/j.est.2019.101061. https://doi.org/10.1016/j.est.2019.101061.